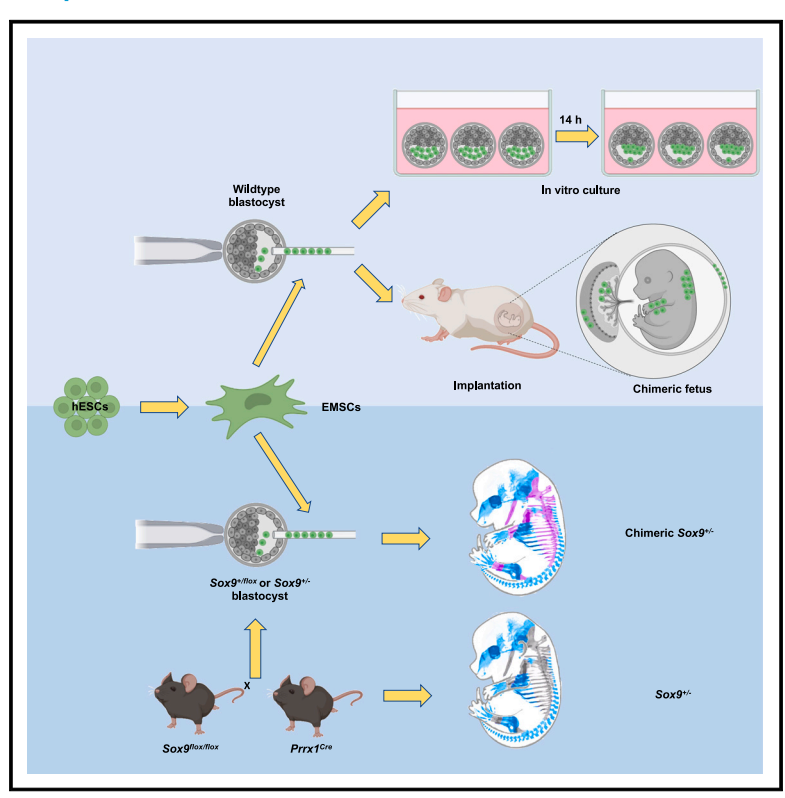
# Developmental potency of human ES cell-derived mesenchymal stem cells revealed in mouse embryos following blastocyst injection

### **Graphical abstract**



### **Authors**

Borong Huang, Siyi Fu, Yanan Hao, ..., Xiaoling Xu, Ningyi Shao, Ren-He Xu

### Correspondence

renhexu@um.edu.mo

### In brief

Huang et al. generate a human-mouse chimera by introducing human embryonic stem cell-derived mesenchymal stem cells (EMSCs) into the mouse blastocyst. EMSCs participate in blastocyst compartment segregation and contribute to both embryonic and extraembryonic tissues including the skeleton, skin, yolk sac, and placenta. EMSCs ameliorate skeletal defects caused by *Sox9* mutation.

### **Highlights**

- Human EMSCs can chimerize with the mouse blastocyst
- EMSCs demonstrate multipotency in vivo, contributing to chimeric embryonic tissues
- EMSCs also contribute to extraembryonic tissues in the chimera
- EMSCs ameliorate skeletal defects in Sox9-mutated fetuses







### **Article**

# Developmental potency of human ES cell-derived mesenchymal stem cells revealed in mouse embryos following blastocyst injection

Borong Huang,<sup>1,2</sup> Siyi Fu,<sup>1,2</sup> Yanan Hao,<sup>1,2</sup> Cheung Kwan Yeung,<sup>1</sup> Xin Zhang,<sup>1</sup> Enqin Li,<sup>1</sup> Xiaoling Xu,<sup>1</sup> Ningyi Shao,<sup>1</sup> and Ren-He Xu<sup>1,3,\*</sup>

<sup>1</sup>Center of Reproduction, Development & Aging, and Institute of Translational Medicine, Faculty of Health Sciences, University of Macau, Taipa, Macau, China

<sup>2</sup>These authors contributed equally

<sup>3</sup>Lead contact

\*Correspondence: renhexu@um.edu.mo https://doi.org/10.1016/j.celrep.2023.113459

### **SUMMARY**

Mesenchymal stem cells (MSCs) are present in almost all the tissues in the body, critical for their homeostasis and regeneration. However, the stemness of MSCs is mainly an *in vitro* observation, and lacking exclusive markers for endogenous MSCs makes it difficult to study the multipotency of MSCs *in vivo*, especially for human MSCs. To address this hurdle, we injected GFP-tagged human embryonic stem cell (hESC)-derived MSCs (EMSCs) into mouse blastocysts. EMSCs survived well and penetrated both the inner cell mass and trophectoderm, correlating to the higher anti-apoptotic capability of EMSCs than hESCs. Injected EMSCs contributed to skeletal, dermal, and extraembryonic tissues in the resultant chimera and partially rescued skeletal defects in  $Sox9^{+/-}$  mouse fetuses. Thus, this study provides evidence for the stemness and developmental capability of human MSCs through chimerization with the mouse blastocyst, serving as a model for studying human mesenchymal and skeletal development.

### **INTRODUCTION**

In mammals, mesenchymal stem cells (MSCs) are derived from the mesoderm and the neural crest (NC) and distributed among various types of parenchymal cells throughout the body. MSCs function as structural supporters, microenvironment regulators, and regenerative contributors. An increasing number of tissues including umbilical cord, amnion, placenta, endometrium, bone marrow, fat, and dental pulp have been found to be rich sources for ex vivo isolation of MSCs. MSCs can differentiate in vitro into various mesenchymal cell lineages including osteocytes, chondrocytes, adipocytes, and smooth muscle cells and even nonmesenchymal cells, e.g., neurons and hepatocytes. Different from other stem cell types, MSCs possess both regenerative and immunomodulatory capabilities; thus they have been used as therapy of autoimmune and inflammatory diseases and injuries in a variety of animal and clinical studies.

MSCs can also be derived from pluripotent stem cells (PSCs) including embryonic stem cells (ESCs) and induced PSCs (iPSCs) via various differentiation routes such as mesenchymal precursors, <sup>5,6</sup> NC cells, <sup>7-12</sup> neuromesodermal progenitors, <sup>13</sup> and other unclear lineages. <sup>14–21</sup> As MSCs can be isolated from the extraembryonic tissue chorion (which mainly contain trophoblasts) of human placenta, <sup>22</sup> we hypothesized and proved that human ESC (hESC)-derived trophoblasts <sup>23</sup> can also differentiate to MSCs. <sup>24</sup> Further, we showed that hESC-derived MSCs

(EMSCs) have therapeutic effects on a series of animal models.<sup>24–30</sup> Due to ethical and technical restrictions, no study has yet elucidated whether human MSCs possess developmental potential *in vivo* starting at an early embryonic stage.

The chimera assay has been used to study the developmental potential of cells, involving injection of test cells into a host embryo mainly at pre-implantation stages.31 It has been recognized that the success rate of chimerism is higher (i.e., more injected cells survive and contribute to the host embryo) when both donor cells and recipient embryo match at their developmental stage than that when the donor and recipient don't match. 32,33 Nevertheless, no clear or convincing explanation has yet been provided for why chimerism fails due to a mismatch. Compared to many other multipotent stem cell types, MSCs possess stronger capability of self-renewal and differentiation. Moreover, like PSCs, MSCs have demonstrated high plasticity, i.e., differentiation to cell lineages from not only the mesoderm but also the other germ layers (such as neurons from the ectoderm and hepatocytes from the endoderm). Based on these, we asked whether chimerization could happen between mouse blastocyst and human embryonic MSCs-a cell type that developmentally occurs much later. If yes, it would allow us to study the development and potency of human MSCs in the mouse fetus.

To test this hypothesis, we injected EMSCs into the mouse blastocyst and found they survived in the mouse blastocyst and formed chimera in post-implantation embryos. In contrast,







hESCs injected into mouse blastocysts were subjected to rapid apoptosis and failed to chimerize with the embryos. The different viability was associated with the higher BCL2 level and hence higher anti-apoptotic capability of EMSCs than those of hESCs. Further, EMSCs contributed widely to mesenchymal derivatives in mouse embryonic and extraembryonic tissues and even the maternal tissue decidua. More interestingly, EMSCs reduced skeletal deformities in the mouse fetus with monoallelic knockout of Sox9, a gene critical for mesenchymal development.

### **RESULTS**

### Integration of EMSCs to the inner cell mass and trophectoderm of mouse blastocyst

Using the Envy hESC line that constitutively expressed green fluorescent protein (GFP),34 we generated EMSCs following our protocol via a trophoblast-like stage<sup>24</sup> (Figure S1A). EMSCs were positive for MSC signature markers CD73, CD44, and CD105 (Figure S1C) and capable of tri-lineage differentiation to adipocyte, chondrocyte, and osteocyte (Figure S1D) based on suggested minimal requirements.35 Figure 1A is a work scheme for chimera assays to test the developmental potential of EMSCs in mouse embryos. First, we injected 10 ~ 15 GFP+ EMSCs (from Envy hESCs) into the cavity, i.e., the blastocoel of the mouse blastocyst (Figure S1E), and injected the vehicle alone as a mock control. The blastocoel reduced its size and embraced the injected cells right after the injection and then gradually resumed its shape after culture in the in vitro culture medium<sup>36</sup> for 14 h during which the injected cells retained spindle-like shape and moved within the blastocoel. By 14 h post injection, a certain number of GFP+ cells integrated into the inner cell mass (ICM), and in some blastocysts, one to two cells penetrated the trophectoderm (TE) (Figure 1B and Video S1). A portion of blastocysts expelled injected cells or stopped development. Overall, the average percentages of injected blastocysts with EMSCs integrated to the ICM, TE, and both ICM and TE, and remaining in the cavity were 44.2%, 21.6%, 18.3%, and 15.8%, respectively (Figure 1C).

To verify the results on EMSCs derived from another hESC line, we differentiated CT3 hESCs<sup>37,38</sup> to EMSCs, transduced them with lentiviral particles for GFP expression, and injected the GFP+ CT3-derived EMSCs into mouse blastocysts. The injected cells, like EMSCs from Envy, mainly migrated to the ICM, TE, or both with a small percentage of the cells left in the blastocoel (Figures 1B and 1C). As a control, Envy hESCs at similar numbers were injected into the mouse blastocyst. In sharp contrast, most injected hESCs rounded up with vesicles forming inside and remained in the cavity (Figures 1B and 1C). Immunostaining demonstrates that some EMSCs resided either above the ICM or adjacent to TE cells, expressing neither the pluripotency marker OCT4 nor the trophectoderm marker CDX2 (Figure 1D). The total numbers of injected cell lines and injected and recovered embryos as well as the percentage of embryos containing GFP<sup>+</sup> cells are shown in a table (Figure 1E). We also generated EMSCs differentiated from hESCs through NC cells (NC-EMSCs) as reported (Figure S1B).39 After characterization (Figures S1C and S1D), we injected NC-EMSCs into the mouse blastocyst. NC-EMSCs persisted and migrated inside the em-

bryo and further resided in the ICM and TE, and some remained in the cavity (blastocoel) during in vitro culture for 14 h (Figure S1F). No activated caspase 3 (aCasp3), an apoptotic marker, was detected in either the injected cells or the embryo after the culture (Figure S1G). Thus, EMSCs obtained via two different intermediate steps both could chimerize with the mouse blastocysts.

### Higher anti-apoptotic property of EMSCs than hESCs

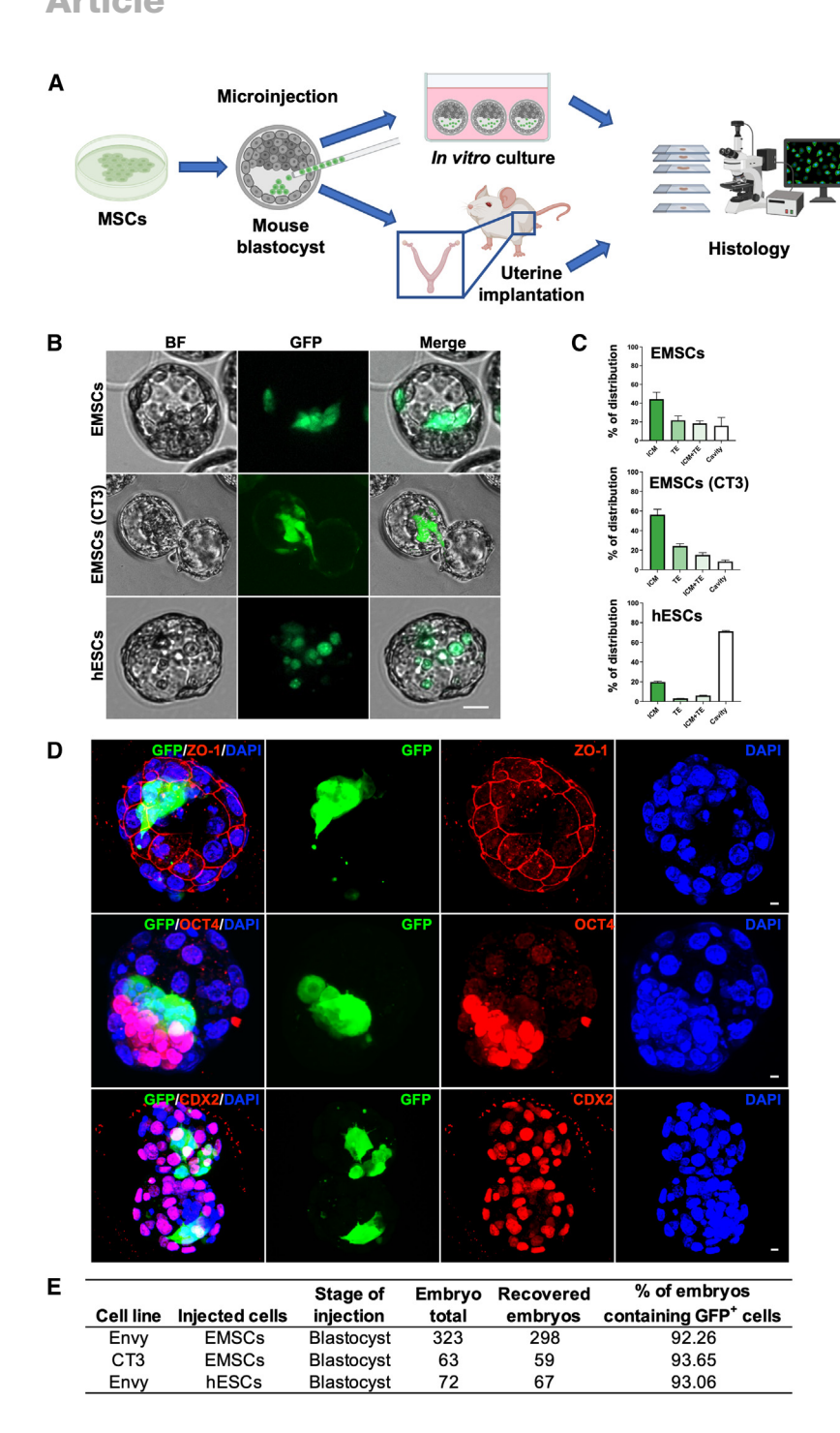
To elucidate the mechanisms for the different outcomes observed above, we detected the levels of anti-apoptotic factor BCL2 and its homolog BCL-XL40,41 in EMSCs. Interestingly, we found that EMSCs expressed a higher level of BCL2 than hESCs (Figures 2A-2C). Consistently, high levels of aCasp3 were detected in injected hESCs, whereas little or no aCasp3 was detected in injected EMSCs (Figure 2D). However, similar levels of BCL-XL were detected in hESCs and EMSCs (Figure 2B). We then constructed four shRNAs to inhibit BCL2 expression and selected #2-4 for BCL2 knockdown (Figures S2A-S2C). Envy (GFP+) EMSCs expressing the BCL2-shRNA survived poorly following injection into the mouse blastocyst and were detected positive for aCasp3 (Figures 2E and S2D), indicating that BCL2 is not dispensable for the survival of injected EMSCs. The name of the injected cell lines and the numbers of injected and recovered embryos as well as the number and percentage of embryos containing aCasp3+ cells are shown in a table (Figures 2F and S2E).

### Contributions of EMSCs to mouse embryonic and extraembryonic tissues

Inspired by the above observations of EMSC-injected mouse blastocysts cultured in vitro, we implanted EMSC-injected blastocysts into the uterine horns of surrogate mice to allow continuous embryogenesis until embryonic day (E)14 and E16 when the resultant fetuses were collected. First, the uteruses were isolated to check the general status of the chimeras. At E14 and E16, EMSC-injected embryos, like mock-injected ones, developed similarly in the uterus. Then the fetus, placenta, and yolk sac were dissected out of the uterine horns under fluorescent stereomicroscope to check for any morphological retardation or developmental defects. Each of the fetuses had normal morphologies and carried a full set of extraembryonic tissues including the placenta, amnion, and yolk sac and did not show any sign of degeneration, oversized growth, or tumorigenesis. Given the thickness and autofluorescence of the fetuses, no specific GFP signal could be identified in the fetuses under stereomicroscope. To study the histological structures and locate human cells in the fetuses, we processed the samples for cryosection and immunofluorescence.

Through immunohistochemistry on sections of E16 fetuses with anti-GFP antibody, we found dozens of GFP+ cells per view in sections of skeletal tissues including the sternum (Figure 3D), ribs (Figure 3C), long bones in the limbs (Figure 3B), and vertebral disks in the spine (Figure 3A). A proportion of GFP+ cells in the sternum and ribs was also positive for SOX9 among mouse Sox9+ cells (Figure S3F), a critical transcription factor for chondrogenesis, indicating the contribution of EMSCs to the chondrocyte population. 42 GFP+ cells were also





found in long bones of the limbs with some positive for SP7 among mouse Sp7+ cells (Figure S3G). SP7, also known as osterix, is an initiating transcription factor for osteogenesis.<sup>43</sup> These data indicate the contributions of EMSCs to both chondrocytes in the rib cage and osteocytes in long bones at this stage. GFP+ cells were also found in the cranial facial bones, although Sox9+ cells were abundant there (Figure S3E). In addition to skeletal tissues, dermis and hypodermis were also destinations of GFP+ cells, although they reached there sparsely

Figure 1. EMSCs chimerize with mouse blastocyst

(A) Scheme of the project workflow.

(B) Mouse blastocysts injected with Envy hESCs or their derived EMSCs or CT3 hESC-derived EMSCs, cultured in vitro, and photographed at 14 h post injection. Scale bar, 25 μm.

(C) Statistical summary of positional integration of the above human cells into various compartments of mouse blastocyst. Experiments were repeated three times (n = 3). Data were displayed as mean  $\pm$ 

(D) Immunostaining for ZO-1, OCT4, and CDX2 on blastocysts injected with EMSCs and cultured in vitro for 14 h. Scale bar, 5 μm.

(E) Summary of recovered embryos injected with hESCs or EMSCs after culture in vitro for 14 h.

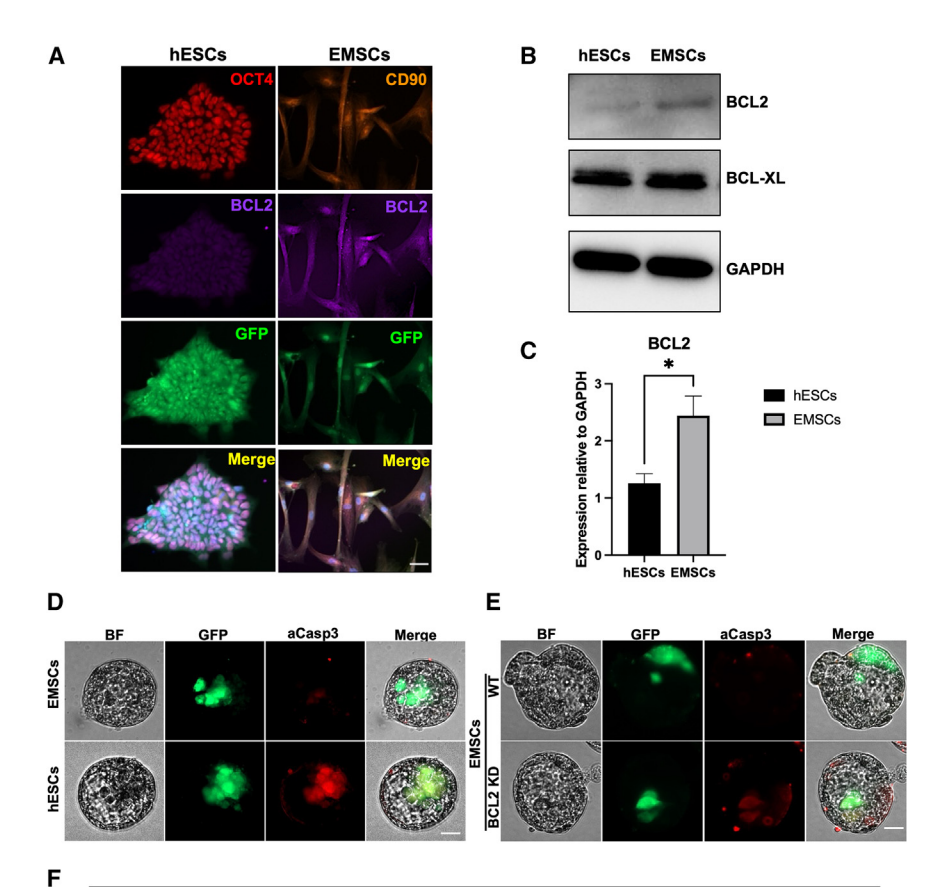
(Figures 3F and S3D). Given all the GFP+ cells were derived from the original 10-15 GFP+ EMSCs injected into each blastocyst, these results suggest that, following injection, EMSCs largely survived, remarkably proliferated, and participated in skeletal and dermal development in the mouse embryo. Nevertheless, no GFP+ signal was detected in the central nervous system or gonads (Figure S3C), which reduces the ethic concern for human cell participation in these organs. To validate the human cell contribution into the chimeras, we detected human thymidine kinase (hTK) gene among total DNA in chimeric embryos at E14 via qPCR assay with a threshold 1/10<sup>5</sup> (Figure 3H). The results correlate with the immunostaining data, confirming the contributions of human cells into the chimeric embryos.

Since injected EMSCs penetrated both ICM (including the epiblasts and hypoblasts) and TE in many blastocysts, we asked whether GFP+ cells would also contribute to extraembryonic tissues. Indeed, GFP+ cells were found in the yolk sac, overlapping with cytokeratin<sup>+</sup> epithelial cells (Figure 3G) but excluded from Pdgfra+ endothelial cells (Figure S3I). GFP+ cells even reached and crossed the fetal-maternal interface as they were found to be mixed with cytokera-

tin+ cells (potentially trophoblasts) in the placenta (Figure S3H) and overlapping with some vimentin+ decidual cells of the maternal uterine (Figure S3J). Consistently, hTK DNA was also detected in the chimeric placentas with a 1/10<sup>5</sup> threshold (Figure 3I).

These results suggest that EMSCs are competent to penetrate almost all the major cell lineages in the mouse blastocyst and further contribute to embryonic, extraembryonic, and even maternal tissues after the blastocyst implantation in a surrogate uterus. Nevertheless, in the chimeric embryo, EMSCs retained





Cell line	Stage of injection	Embryo total	Recovered embryos	# of aCasp3 <sup>+</sup> embryo	% of embryos containing aCasp3 <sup>+</sup> cells
EMSCs	Blastocyst	62	59	0	0.00
hESCs	Blastocyst	47	46	45	97.83
BCL2-KD EMSCs(#2)	Blastocyst	52	45	32	71.11

their mesenchymal nature as they mainly differentiated to chondrocytes and osteocytes in the fetus as detected by this stage.

### Partial rescue of skeletal defects in Sox9<sup>+/-</sup> mouse fetuses by injected EMSCs

Since EMSCs and their progeny widely integrated into the skeletal tissues of the mouse fetus and many of the cells (GFP+) expressed the critical chondrogenic marker SOX9, we asked whether EMSCs can rescue skeletal defects in the mouse model with mutated Sox9. Bone development during embryogenesis mainly consists of three steps: mesenchymal condensation, chondrogenic differentiation, and replacement of chondrocytes with osteocytes. 44 Sox9 promotes chondrogenesis, and systematic double knockout of Sox9 ( $Sox9^{-/-}$ ) in mice is embryonically lethal by E11.5<sup>45</sup> Double knockout of Sox9 specifically in mesenchymal lineages through crossing of Prrx1-Cre:Sox9<sup>flox/-</sup> mouse strains leads to poor or absent chondrogenesis and osteogenesis, reflected by the lack of limb formation, severe bending of vertebra, and shrunken thorax mouse fetuses. 46 Even crossing Prrx1-Cre:Sox9<sup>flox/-</sup> with Sox9<sup>+/+</sup> also led to mostly dead and absorbed embryos per our observations. Therefore, we employed

Figure 2. High anti-apoptotic activity is critical for the chimerizing capability of EMSCs

(A) Immunostaining for anti-apoptotic factors BCL-2 in hESCs and EMSCs. Scale bar, 25 µm. (B) Western blotting for anti-apoptotic factors BCL-2 and BCL-XL in hESCs and EMSCs.

(C) Quantification of BCL2 protein level relative to GAPDH based on three western blotting experiments as above. Data are displayed as mean  $\pm$ SEM. \*p < 0.05, n = 3.

(D) Immunostaining for aCasp3 in Envy hESCs or EMSCs in mouse blastocysts following culture in vitro for 14 h. Scale bar. 25 um.

(E) Immunostaining for aCasp3 in fixed embryos injected with BCL2-KD EMSCs and cultured in vitro for 14 h. The zona of the embryos was removed before immunostaining. Scale bar,  $25~\mu m$ . Representative embryos are shown.

(F) Summary of recovered embryos injected with various human cells and detected for aCasp3+ cells after culture in vitro for 14 h.

a milder model by crossing Sox9<sup>flox/flox</sup> and Prrx1-Cre strains to obtain conditionally Sox9 knockout in one allele (Sox9 $^{+/-}$ ) in mesenchymal lineages (Figure 4A) as reported previously46 and conducted whole-skeleton staining of the resultant fetuses at E16.

As expected, Sox9+/- fetuses had obviously retarded skeleton, including shortened iawbone, reduced chondrogenic condensation in the cranial bone and thorax, and decreased chondrogenesis and osteogenesis in vertebral discs and limbs compared to Sox9flox/flox fetuses (Figures 4B and S4A). EMSC injection at the blastocyst stage remarkably relieved the

defects in  $Sox9^{+/-}$  fetuses. In the E16  $Sox9^{flox/flox}$  fetuses, the cranial facial bones, radius, and ulnas in the forelimbs, ribs, spine, and hindlimbs have the typical patterns of mineralized segment stained purple by Alizarin red (pointed by arrowheads in Figure 4B), and cartilages in the skeleton stained blue by Alcian blue. In Sox9<sup>+/-</sup> fetus, the skeletal bones appeared somehow transparent due to poor mineralization. Chimerization with EMSCs ameliorated the defects by increasing the mineralization (Figures 4C and 4D). Statistics analysis was performed by quantifying (via ImageJ) and comparing the mineralized (purple) areas in the head, forelimbs, and hindlimbs in the Sox9<sup>flox/flox</sup>, Sox9<sup>+/-</sup> and Sox9<sup>+/-</sup> + EMSCs fetuses (Figure 4E). Partially rescued chondrogenesis in the ribs of EMSC-injected Sox9+/- fetuses are highlighted in magnified images (Figures 4C and 4D) and morphologically verified via histological analysis of the ribs following vertical sections (Figure S4B). hTK DNA was detected in all the surviving chimeric embryos (Figure 4F) but slightly less among the chimeric placentas with a 1/10<sup>5</sup> threshold (Figure S4C). These data suggest that EMSCs injected into Sox9+/- mouse blastocysts can also contribute to both the embryonic and extraembryonic tissues and partially rescue the skeletal defects in resultant fetuses.



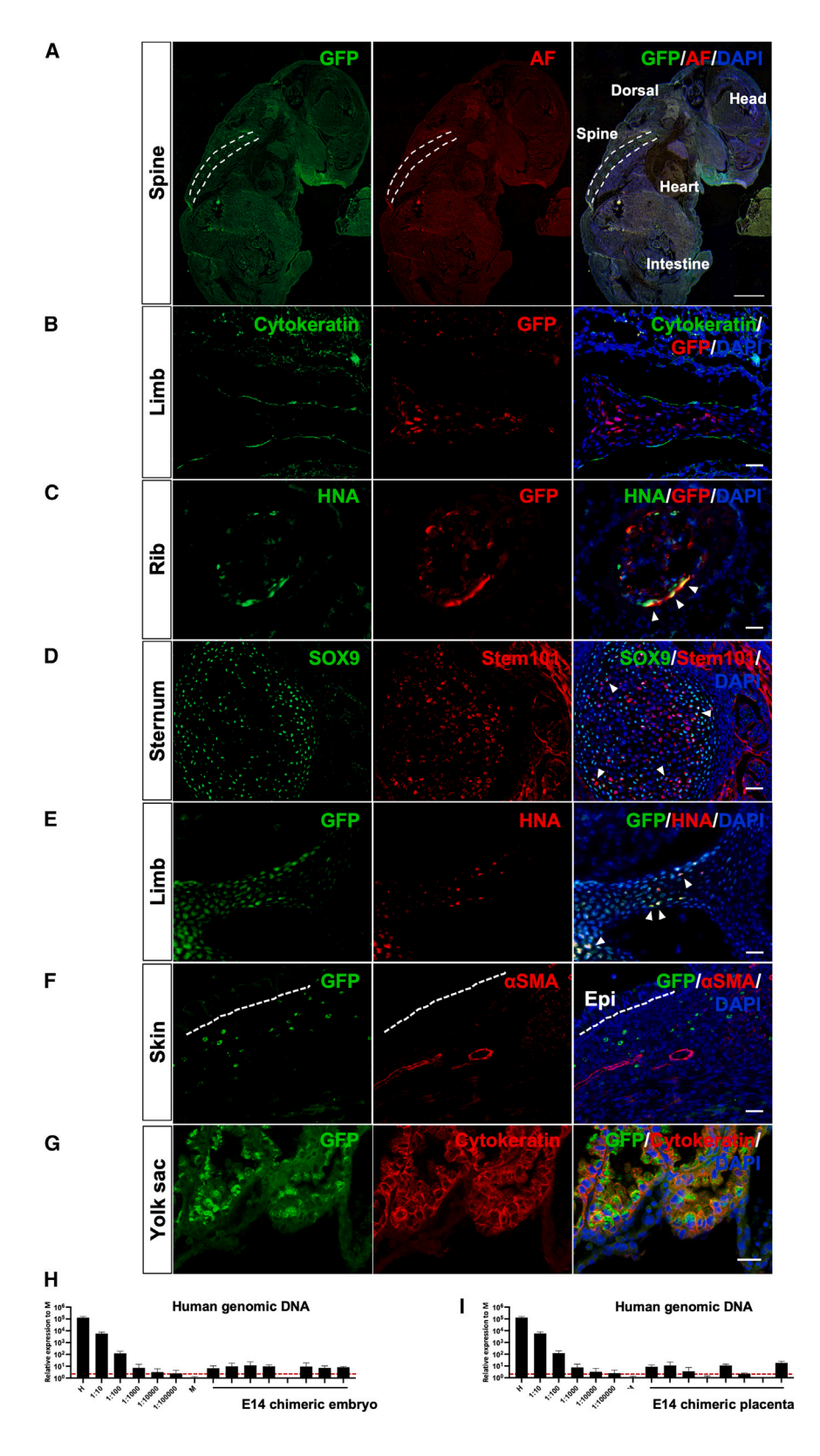


Figure 3. Contributions of EMSCs to skeletal and extraembryonic tissues in E16 mouse fetus

Positional schemes of section planes are shown on the left and immunofluorescent images on the right. Cellular nuclei were counterstained with DAPI in some sections.

- (A) The sagittal plane of a chimera immunostained with an anti-GFP antibody conjugated with FITC fluorophore. The dashed lines mark the real positive signals for human cells in the spine. Scale bar,
- (B) Detection of GFP+ cells in the limb and costained for pan-cytokeratin. Scale bar, 25 μm.
- (C) Detection of GFP+ cells in a rib and co-stained for human nuclear antigen (HNA). Scale bar,
- (D) Detection of Stem101+ and Sox9+ cells in the sternum. Scale bar, 25 µm.
- (E) Detection of HNA+ and GFP+ cells in the limb. Scale bar, 25  $\mu m$ .
- (F) Detection of GFP $^+$  and  $\alpha$ SMA $^+$  cells in the skin. Scale bar, 25 μm. (G) Detection of GFP<sup>+</sup> and pancytokeratin+ cells in the epithelial layer of the yolk sac. Scale bar, 25 μm.
- (H and I) qPCR-based detection of human genomic DNA in E14 chimeric embryos (H) and placentas (I). Data were displayed as mean ±



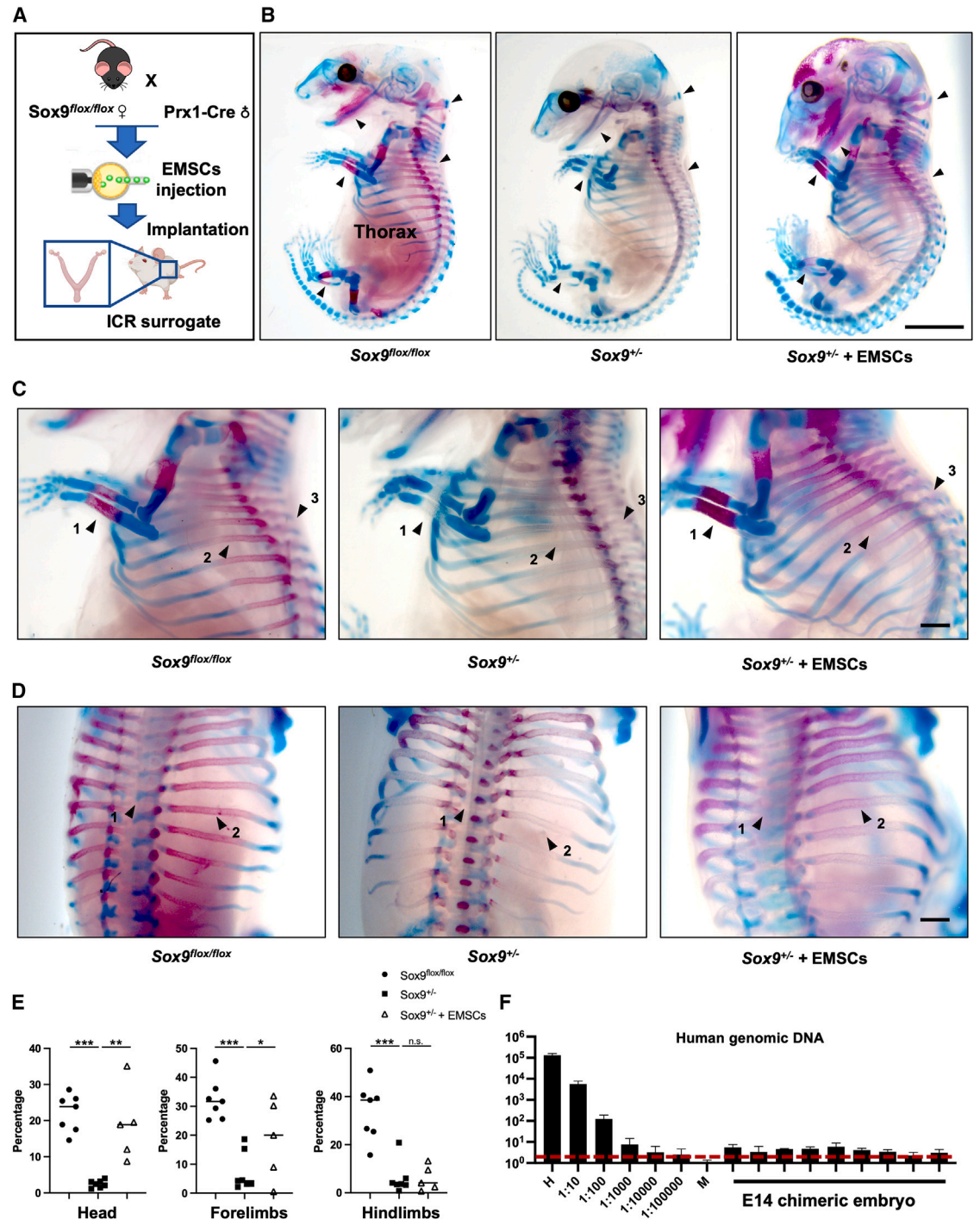


Figure 4. Partial rescue of skeletal defects in Sox9-mutated, E16 mouse fetus by EMSCs

(A) Scheme for the experiment. Blastocysts generated from crossing Sox9<sup>flox/flox</sup> (?) and Prrx1-Cre (3) were injected with EMSCs, followed by implantation into the uterus of a surrogate mouse to produce Sox9+/- fetuses.

- (B) Skeletal images of E16 fetuses derived from Sox9<sup>flox/flox</sup> and Sox9<sup>+/-</sup> blastocysts and Sox9<sup>+/-</sup> blastocyst injected with EMSCs. Scale bar, 2.5 mm. Mineralized osteocytes were stained purple with Alizarin red (pointed by arrowheads) and chondrocytes stained blue with Alician blue.
- (C) Zoom-in views of above for the forelimbs, thorax, and spine with mineralized areas indicated by arrows. Arrow 1 points to the radius and ulnas, arrow 2 to the dorsal segment of a rib, and arrow 3 to the vertebral column. Scale bar, 2.5 mm.
- (D) Dorsal view of the rib cage of the above fetuses. Arrow 1 points to a vertebral disc and arrow 2 to a rib. Scale bar, 2.5 mm.
- (E) Quantification of purple (Alizarin red\*) areas in the head, forelimb, and hindlimb via ImageJ, displayed as percent of the mineralized regions. \*p < 0.05, \*\*p < 0.01, \*\*\*p < 0.001, and n.s., not significant.
- (F) qPCR-based detection of human genomic DNA in E14  $Sox9^{+/-}$  chimeric embryos. Data were displayed as mean  $\pm$  SEM.

### **Article**



### **DISCUSSION**

In this study, we have demonstrated that EMSCs derived from either trophoblasts or NC cells were able to survive in mouse embryo following blastocyst injection and to further develop and contribute to skeletal and dermal tissues in the fetus and even to the yolk sac, placenta, and uterine decidua. Moreover, EMSCs partially corrected skeletal defects in Sox9<sup>+/-</sup> mouse fetuses. Many of the findings are unexpected based on the current

According to the epigenetic landscape proposed by Conrad Hal Waddington,<sup>47</sup> a cell like EMSC that has been differentiated "downhill" possesses much reduced competence than cells in a blastocyst that are near the "mountaintop" of the embryogenesis. Thus, it has been widely recognized that developmental compatibility is a crucial factor for chimera formation. 32,33 In sharp contrast, we provide evidence here that human EMSCs can form interspecies chimera with mouse blastocyst. This suggests that EMSCs can adapt to the microenvironment in the mouse blastocyst due to their high plasticity.<sup>48</sup>

As described above, the multipotency or stemness of MSCs is largely observed in vitro and difficult to prove in vivo because of the lack of exclusive markers for MSCs. Great efforts have been made to track the development and differentiation of endogenous cells with MSC properties in mice, which were found to be mainly pericytes. 42,49 On the other hand, it has been shown that human bone marrow MSCs, following intraperitoneal (i.p.) injection into fetal sheep at either 65 or 85 days of gestation, undergo site-specific differentiation into chondrocytes, adipocytes, myocytes, and cardiomyocytes, marrow stromal cells, and thymic stroma and persisted in multiple tissues for as long as 13 months. 50 The two injection dates correspond to the times before and after the development of immunocompetence, respectively, in the fetal sheep, and MSCs have unique immunologic characteristics that allow persistence in a xenogeneic environment.

We conducted interspecies transplantation at the blastocyst stage of the host with a big time window (up to 14 h) to observe the developmental process of a chimera in vitro. EMSCs succeeded to chimerize with mouse blastocyst and to contribute to multiple skeletal tissues including the sternum, ribs, limbs, and vertebral disks as well as dermal tissues, lending strong support for the multipotency or stemness of external MSCs in a host embryo via transplantation at the blastocyst stage. It has been suggested that endogenous MSCs are often present in perivascular sites and express PDGFRa.51 However, we didn't find EMSCs or their derivatives expressing PDGFRα in the tested tissues (Figure S3I), indicating that EMSCs might have largely differentiated to other cell types rather than perivascular MSCs in the chimeric fetus.

Through fetal-to-fetal transplantation, it has been found that external MSCs can compensate for skeletal defects in a host. For example, Fisk and coworkers treated mouse fetus with X-linked muscular dystrophy (mdx) with human fetal MSCs via i.p. injection at E14-16 and observed widespread distribution and muscle differentiation of human MSCs in the offspring, although it was not curative for the disease. 52 They also treated mouse fetus with another genetic disease osteogenesis imperfecta via i.p. injection of human fetal MSCs at E13.5-E15, which reduced fractures in the offspring.<sup>53</sup> In this study, EMSCs injected into mouse blastocyst remarkably corrected skeletal defects caused by Sox9 mutation in the chimeric fetus.

Any competent cell injected into the blastocyst may face the choice of three cell lineages: the hypoblast, epiblast, and TE. Theoretically, MSCs don't belong to any of the lineages, thus shouldn't possess preference to any of the three locations. However, we observed that EMSCs not only migrated to the ICM including the epiblast and hypoblast but also the TE. EMSCs contributed to not only the embryo proper (derived from the epiblast) but also the extraembryonic tissues including the yolk sac (derived from the hypoblast) and placenta (derived from the TE) and even the decidua of the uterus. The transient shrinking of the mouse blastocyst following EMSC injection might give a chance for EMSCs to penetrate any nearby host cell lineages.

Through immunohistochemistry, we noticed three destinations of EMSCs in the following extraembryonic tissues and beyond at E16. (1) Placenta. GFP+ human cells were detected in the placenta through immunohistochemistry and gPCR and co-stained for only the pan-cytokeratin, a marker for multiple epithelial tissues (Figure S3), but not trophoblast markers cytokeratin 7 and Tfap2c, and the vascular endothelial marker CD31. Therefore, EMSCs that reached the placenta might have just experienced mesenchymal-epithelial transition but not yet fully determined their fate. (2) Yolk sac. Human cells detected there didn't overlap with the mesenchymal marker Pdgfrα (Figure S3I) but again were positive for pan-cytokeratin (Figure 3G), indicating a status like above. (3) Decidua. Dozens of EMSCs migrated to the decidua and retained their mesenchymal nature based on their positivity for vimentin. These extraembryonic contributions might result from both the invasiveness and plasticity of EMSCs in the xenogeneic environment.

As described above, inhibiting apoptosis via ectopic expression of BCL2 or BMI1 allows hPSCs, following injection into mouse blastocyst, to contribute to not only embryonic tissues derived from all the three germ layers but also extraembryonic tissues including the placenta and yolk sac as observed by E10.5.40,54 Using four small chemicals, Deng and coworkers converted primed hPSCs to extended pluripotent stem (EPS) cells, and one EPS cell could chimerize both embryonic and extraembryonic tissues as of E10.5.55 Although much lower in potency than PSCs and EPS cells, EMSCs could still differentiate to chondrocytes, osteocytes, and other cells in the fetus as of E16 and mix with epithelial cells in the yolk sac, trophoblasts in the placenta, and even decidual cells in the uterus. This capability highlights the plasticity and invasiveness of EMSCs in the embryonic environment.

### Limitations of the study

Given the above findings revealed in this study, some important questions remain to be addressed. (1) It awaits further study for how EMSCs possess or gain the capability to chimerize with the mouse blastocyst. Although RNA-seq on EMSC-injected embryos demonstrated transcriptomic alternations of EMSCs (Figures S2F-S2M), spatio-temporal single-cell RNA sequencing is needed to address the fate change and mechanism for the chimerism. (2) Although the resistance to apoptosis was found





to be crucial for the chimerizing capability of EMSCs in mouse blastocyst, it is possible that other mechanisms are also involved, which may be revealed via in-depth studies of injected cells. (3) Due to the limitation of immunostaining (for GFP), we can't assure the detection of EMSCs and their derivatives if they existed scarcely in other tissues, which demands more robust and precise methods. (4) Ethical restrictions prohibit the birth of the chimeras, so we cannot investigate the continuous development and tissue-specific functions of EMSCs and their derivatives in postnatal mice and their offspring. Nevertheless, this study has provided evidence that chimera formation is possible between mouse blastocyst and multipotent human MSCs. It may serve as a model for studying human mesenchymal and skeletal development and a platform for human skeletal organogenesis for clinical applications.

### **STAR**\*METHODS

Detailed methods are provided in the online version of this paper and include the following:

- KEY RESOURCES TABLE
- RESOURCE AVAILABILITY
  - Lead contact
  - Materials availability
  - Data and code availability
- EXPERIMENTAL MODEL AND STUDY PARTICIPANT DE-**TAILS** 
  - Ethics statement
  - Mice
- METHOD DETAILS
  - hESC culture and MSC generation
  - Blastocyst isolation and microinjection
  - Embryo implantation
  - In vitro culture of mouse embryos
  - Whole-mount embryo staining and imaging
  - Histological analysis
  - Whole-mount skeleton staining
  - Genotyping
  - Knockdown assay with lentiviral vectors
  - Western blotting
  - O Trilineage differentiation of MSCs
  - Flow cytometry
  - Bulk RNA-seq and analysis
- QUANTIFICATION AND STATISTICAL ANALYSIS

### SUPPLEMENTAL INFORMATION

Supplemental information can be found online at https://doi.org/10.1016/j. celrep.2023.113459.

### **ACKNOWLEDGMENT**

We thank all the core facilities in the Faculty of Health Sciences, especially the Animal Research Core and the Bioimaging and Stem Cell Core, for their excellent services. This work was supported with the National Key R&D Program of China no. 2022YFA1105000, University of Macau Research Committee funds nos. CPG2021-00031-FHS and CPG2023-00009-FHS, MYRG #2020-00140-FHS and 2022-00044-FHS, Macau Science and Technology Development Fund (FDCT) Key grant no. 0002/2021/AKP and general grant no. 0071/

2022/A2, and National Natural Science Foundation of China general grant no. 32270842 to R.X. The authors thank Linzhao Cheng and the council members of the Macau Society for Stem Cell Research for helpful discussion.

### **AUTHOR CONTRIBUTIONS**

R.-H.X. and B.H. conceived of and designed the research. B.H., S.F., X.Z., C.K.Y., and E.L. performed the experiments. B.H., S.F., X.X., Y.H., N.S., and R.-H.X. analyzed all the data. B.H. and R.-H.X. wrote the manuscript. R.-H.X. gave the final approval of the manuscript.

### **DECLARATION OF INTERESTS**

R.-H.X. is a founder of ImStem Biotechnology, Inc., a stem cell company.

### **INCLUSION AND DIVERSITY**

We support inclusive, diverse, and equitable conduct of research.

Received: March 3, 2023 Revised: August 26, 2023 Accepted: November 2, 2023

### **REFERENCES**

- 1. Soliman, H., Theret, M., Scott, W., Hill, L., Underhill, T.M., Hinz, B., and Rossi, F.M.V. (2021). Multipotent stromal cells: One name, multiple identities. Cell Stem Cell 28, 1690-1707.
- 2. Bianco, P. (2014). "Mesenchymal" Stem Cells. Annu. Rev. Cell Dev. Bi. 30, 677-704.
- 3. Caplan, A.I. (1991). Mesenchymal stem cells. J. Orthop. Res. 9, 641–650.
- 4. Wang, Y., Chen, X., Cao, W., and Shi, Y. (2014). Plasticity of mesenchymal stem cells in immunomodulation: pathological and therapeutic implications. Nat. Immunol. 15, 1009-1016.
- 5. Vodyanik, M.A., Yu, J., Zhang, X., Tian, S., Stewart, R., Thomson, J.A., and Slukvin, II. (2010). A mesoderm-derived precursor for mesenchymal stem and endothelial cells. Cell Stem Cell 7, 718-729.
- 6. Guzzo, R.M., Scanlon, V., Sanjay, A., Xu, R.H., and Drissi, H. (2014). Establishment of human cell type-specific iPS cells with enhanced chondrogenic potential. Stem Cell Rev. Rep. 10, 820-829.
- 7. Takashima, Y., Era, T., Nakao, K., Kondo, S., Kasuga, M., Smith, A.G., and Nishikawa, S. (2007). Neuroepithelial cells supply an initial transient wave of MSC differentiation. Cell 129, 1377-1388.
- 8. Morikawa, S., Mabuchi, Y., Niibe, K., Suzuki, S., Nagoshi, N., Sunabori, T., Shimmura, S., Nagai, Y., Nakagawa, T., Okano, H., and Matsuzaki, Y. (2009). Development of mesenchymal stem cells partially originate from the neural crest. Biochem. Bioph Res. Co. 379, 1114-1119.
- 9. Lee, G., Chambers, S.M., Tomishima, M.J., and Studer, L. (2010). Derivation of neural crest cells from human pluripotent stem cells. Nat. Protoc. 5, 688-701.
- 10. Menendez, L., Kulik, M.J., Page, A.T., Park, S.S., Lauderdale, J.D., Cunningham, M.L., and Dalton, S. (2013). Directed differentiation of human pluripotent cells to neural crest stem cells. Nat. Protoc. 8, 203-212.
- 11. Menendez, L., Yatskievych, T.A., Antin, P.B., and Dalton, S. (2011). Wnt signaling and a Smad pathway blockade direct the differentiation of human pluripotent stem cells to multipotent neural crest cells. Proc. Natl. Acad. Sci. USA 108. 19240-19245.
- 12. Fukuta, M., Nakai, Y., Kirino, K., Nakagawa, M., Sekiguchi, K., Nagata, S., Matsumoto, Y., Yamamoto, T., Umeda, K., Heike, T., et al. (2014). Derivation of Mesenchymal Stromal Cells from Pluripotent Stem Cells through a Neural Crest Lineage using Small Molecule Compounds with Defined Media. PLoS One 9, ARTN e112291.

### **Article**



- 13. Wang, H., Li, D., Zhai, Z., Zhang, X., Huang, W., Chen, X., Huang, L., Liu, H., Sun, J., Zou, Z., et al. (2019). Characterization and Therapeutic Application of Mesenchymal Stem Cells with Neuromesodermal Origin from Human Pluripotent Stem Cells. Theranostics 9, 1683-1697.
- 14. Olivier, E.N., Rybicki, A.C., and Bouhassira, E.E. (2006). Differentiation of human embryonic stem cells into bipotent mesenchymal stem cells. Stem Cell 24, 1914-1922.
- 15. Sheyn, D., Ben-David, S., Shapiro, G., de Mel, S., Bez, M., Ornelas, L., Sahabian, A., Sareen, D., Da, X.Y., Pelled, G., et al. (2016). Human Induced Pluripotent Stem Cells Differentiate Into Functional Mesenchymal Stem Cells and Repair Bone Defects. Stem Cell Transl. Med. 5, 1447–1460.
- 16. Giuliani, M., Oudrhiri, N., Noman, Z.M., Vernochet, A., Chouaib, S., Azzarone, B., Durrbach, A., and Bennaceur-Griscelli, A. (2011). Human mesenchymal stem cells derived from induced pluripotent stem cells down-regulate NK-cell cytolytic machinery. Blood 118, 3254-3262.
- 17. Karlsson, C., Emanuelsson, K., Wessberg, F., Kajic, K., Axell, M.Z., Eriksson, P.S., Lindahl, A., Hyllner, J., and Strehl, R. (2009). Human embryonic stem cell-derived mesenchymal progenitors-Potential in regenerative medicine. Stem Cell Res. 3, 39-50.
- 18. Liu, Y.X., Goldberg, A.J., Dennis, J.E., Gronowicz, G.A., and Kuhn, L.T. (2012). One-Step Derivation of Mesenchymal Stem Cell (MSC)-Like Cells from Human Pluripotent Stem Cells on a Fibrillar Collagen Coating. PLoS One 7, e33225, ARTN,
- 19. Li, O., Tormin, A., Sundberg, B., Hyllner, J., Le Blanc, K., and Scheding, S. (2013). Human embryonic stem cell-derived mesenchymal stroma cells (hES-MSCs) engraft in vivo and support hematopoiesis without suppressing immune function: implications for off-the shelf ES-MSC therapies. PLoS One 8, e55319.
- 20. Wei, Y., Hou, H., Zhang, L., Zhao, N., Li, C., Huo, J., Liu, Y., Zhang, W., Li, Z., Liu, D., et al. (2019). JNKi- and DAC-programmed mesenchymal stem/ stromal cells from hESCs facilitate hematopoiesis and alleviate hind limb ischemia. Stem Cell Res. Ther. 10, 186.
- 21. Hass, R., Kasper, C., Bohm, S., and Jacobs, R. (2011). Different populations and sources of human mesenchymal stem cells (MSC): A comparison of adult and neonatal tissue-derived MSC. Cell Commun. Signal. 9, 12.
- 22. Xu, R.H., Chen, X., Li, D.S., Li, R., Addicks, G.C., Glennon, C., Zwaka, T.P., and Thomson, J.A. (2002). BMP4 initiates human embryonic stem cell differentiation to trophoblast. Nat. Biotechnol. 20, 1261-1264.
- 23. Wang, X., Lazorchak, A.S., Song, L., Li, E., Zhang, Z., Jiang, B., and Xu, R.H. (2016). Immune modulatory mesenchymal stem cells derived from human embryonic stem cells through a trophoblast-like stage. Stem Cell 34, 380-391.
- 24. Jiang, B., Fu, X., Yan, L., Li, S., Zhao, D., Wang, X., Duan, Y., Yan, Y., Li, E., Wu, K., et al. (2019). Transplantation of human ESC-derived mesenchymal stem cell spheroids ameliorates spontaneous osteoarthritis in rhesus macaques. Theranostics 9, 6587-6600.
- 25. Jiang, B., Yan, L., Miao, Z., Li, E., Wong, K.H., and Xu, R.H. (2017). Spheroidal formation preserves human stem cells for prolonged time under ambient conditions for facile storage and transportation. Biomaterials 133, 275-286.
- 26. Jiang, B., Yan, L., Wang, X., Li, E., Murphy, K., Vaccaro, K., Li, Y., and Xu, R.H. (2019). Concise Review: Mesenchymal Stem Cells Derived from Human Pluripotent Cells, an Unlimited and Quality-Controllable Source for Therapeutic Applications. Stem Cell 37, 572-581.
- 27. Wang, X., Jiang, B., Sun, H., Zheng, D., Zhang, Z., Yan, L., Li, E., Wu, Y., and Xu, R.H. (2019). Noninvasive application of mesenchymal stem cell spheres derived from hESC accelerates wound healing in a CXCL12-CXCR4 axis-dependent manner. Theranostics 9, 6112-6128.
- 28. Yan, L., Jiang, B., Niu, Y., Wang, H., Li, E., Yan, Y., Sun, H., Duan, Y., Chang, S., Chen, G., et al. (2018). Intrathecal delivery of human ESCderived mesenchymal stem cell spheres promotes recovery of a primate multiple sclerosis model. Cell Death Discov. 4, 28.

- 29. Borkar, R., Wang, X., Zheng, D., Miao, Z., Zhang, Z., Li, E., Wu, Y., and Xu, R.-H. (2021). Human ESC-derived MSCs enhance fat engraftment by promoting adipocyte reaggregation, secreting CCL2 and mobilizing macrophages. Biomaterials 272, 120756.
- 30. Wu, J., Greely, H.T., Jaenisch, R., Nakauchi, H., Rossant, J., and Belmonte, J.C. (2016). Stem cells and interspecies chimaeras. Nature 540 51-59
- 31. Wu, J., Platero-Luengo, A., Sakurai, M., Sugawara, A., Gil, M.A., Yamauchi, T., Suzuki, K., Bogliotti, Y.S., Cuello, C., Morales Valencia, M., et al. (2017). Interspecies Chimerism with Mammalian Pluripotent Stem Cells. Cell 168, 473-486,e415.
- 32. Cohen, M.A., Markoulaki, S., and Jaenisch, R. (2018). Matched Developmental Timing of Donor Cells with the Host Is Crucial for Chimera Formation. Stem Cell Rep. 10, 1445-1452.
- 33. Costa, M., Dottori, M., Ng, E., Hawes, S.M., Sourris, K., Jamshidi, P., Pera, M.F., Elefanty, A.G., and Stanley, E.G. (2005). The hESC line Envy expresses high levels of GFP in all differentiated progeny. Nat. Methods 2,
- 34. Dominici, M., Le Blanc, K., Mueller, I., Slaper-Cortenbach, I., Marini, F., Krause, D., Deans, R., Keating, A., Prockop, D., and Horwitz, E. (2006). Minimal criteria for defining multipotent mesenchymal stromal cells. The International Society for Cellular Therapy position statement. Cytotherapy 8. 315-317.
- 35. Bedzhov, I., Leung, C.Y., Bialecka, M., and Zernicka-Goetz, M. (2014). In vitro culture of mouse blastocysts beyond the implantation stages. Nat. Protoc. 9, 2732-2739.
- 36. Martins-Taylor, K., Nisler, B.S., Taapken, S.M., Compton, T., Crandall, L., Montgomery, K.D., Lalande, M., and Xu, R.H. (2011). Recurrent copy number variations in human induced pluripotent stem cells. Nat. Biotechnol.
- 37. Lin, G., Martins-Taylor, K., and Xu, R.H. (2010). Human embryonic stem cell derivation, maintenance, and differentiation to trophoblast. Methods Mol. Biol. 636, 1-24.
- 38. Stebbins, M.J., Gastfriend, B.D., Canfield, S.G., Lee, M.S., Richards, D., Faubion, M.G., Li, W.J., Daneman, R., Palecek, S.P., and Shusta, E.V. (2019). Human pluripotent stem cell-derived brain pericyte-like cells induce blood-brain barrier properties. Sci. Adv. 5, eaau7375.
- 39. Wang, X., Li, T., Cui, T., Yu, D., Liu, C., Jiang, L., Feng, G., Wang, L., Fu, R., Zhang, X., et al. (2018). Human embryonic stem cells contribute to embryonic and extraembryonic lineages in mouse embryos upon inhibition of apoptosis. Cell Res. 28, 126-129.
- 40. Masaki, H., Kato-Itoh, M., Takahashi, Y., Umino, A., Sato, H., Ito, K., Yanagida, A., Nishimura, T., Yamaguchi, T., Hirabayashi, M., et al. (2016). Inhibition of Apoptosis Overcomes Stage-Related Compatibility Barriers to Chimera Formation in Mouse Embryos. Cell Stem Cell 19, 587-592.
- 41. Akiyama, H., Kim, J.E., Nakashima, K., Balmes, G., Iwai, N., Deng, J.M., Zhang, Z., Martin, J.F., Behringer, R.R., Nakamura, T., and de Crombrugghe, B. (2005). Osteo-chondroprogenitor cells are derived from Sox9 expressing precursors. Proc Natl Acad Sci USA 102, 14665–14670.
- 42. Kaback, L.A., Soung do, Y., Naik, A., Smith, N., Schwarz, E.M., O'Keefe, R.J., and Drissi, H. (2008). Osterix/Sp7 regulates mesenchymal stem cell mediated endochondral ossification. J. Cell. Physiol. 214, 173-182.
- 43. Gilbert, S.F., and Barresi, M.J.F. (2016). Developmental Biology, Eleventh edition (Sinauer Associates, Inc.).
- 44. Barrionuevo, F., Bagheri-Fam, S., Klattig, J., Kist, R., Taketo, M.M., Englert, C., and Scherer, G. (2006). Homozygous inactivation of Sox9 causes complete XY sex reversal in mice. Biol. Reprod. 74, 195-201.
- 45. Akiyama, H., Chaboissier, M.C., Martin, J.F., Schedl, A., and de Crombrugghe, B. (2002). The transcription factor Sox9 has essential roles in successive steps of the chondrocyte differentiation pathway and is required for expression of Sox5 and Sox6. Genes Dev. 16, 2813-2828.
- 46. Waddington, C.H. (1957). The Strategy of the Genes; a Discussion of Some Aspects of Theoretical Biology (Allen & Unwin)).





- 47. Zheng, C., Hu, Y., Sakurai, M., Pinzon-Arteaga, C.A., Li, J., Wei, Y., Okamura, D., Ravaux, B., Barlow, H.R., Yu, L., et al. (2021). Cell competition constitutes a barrier for interspecies chimerism. Nature 592, 272-276.
- 48. Miwa, H., and Era, T. (2018). Tracing the destiny of mesenchymal stem cells from embryo to adult bone marrow and white adipose tissue via Pdgfralpha expression. Development 145.
- 49. Liechty, K.W., MacKenzie, T.C., Shaaban, A.F., Radu, A., Moseley, A.M., Deans, R., Marshak, D.R., and Flake, A.W. (2000). Human mesenchymal stem cells engraft and demonstrate site-specific differentiation after in utero transplantation in sheep. Nat. Med. 6, 1282-1286.
- 50. Farahani, R.M., and Xaymardan, M. (2015). Platelet-Derived Growth Factor Receptor Alpha as a Marker of Mesenchymal Stem Cells in Development and Stem Cell Biology. Stem Cells Int. 2015, 362753.
- 51. Chan, J., Waddington, S.N., O'Donoghue, K., Kurata, H., Guillot, P.V., Gotherstrom, C., Themis, M., Morgan, J.E., and Fisk, N.M. (2007). Widespread distribution and muscle differentiation of human fetal mesenchymal stem cells after intrauterine transplantation in dystrophic mdx mouse. Stem Cell 25, 875-884.
- 52. Guillot, P.V., Abass, O., Bassett, J.H., Shefelbine, S.J., Bou-Gharios, G., Chan, J., Kurata, H., Williams, G.R., Polak, J., and Fisk, N.M. (2008). Intrauterine transplantation of human fetal mesenchymal stem cells from firsttrimester blood repairs bone and reduces fractures in osteogenesis imperfecta mice. Blood 111, 1717-1725.
- 53. Huang, K., Zhu, Y., Ma, Y., Zhao, B., Fan, N., Li, Y., Song, H., Chu, S., Ouyang, Z., Zhang, Q., et al. (2018). BMI1 enables interspecies chimerism with human pluripotent stem cells. Nat. Commun. 9, 4649.
- 54. Yang, Y., Liu, B., Xu, J., Wang, J., Wu, J., Shi, C., Xu, Y., Dong, J., Wang, C., Lai, W., et al. (2017). Derivation of Pluripotent Stem Cells with In Vivo Embryonic and Extraembryonic Potency. Cell 169, 243-257.e25.
- 55. Daley, G.Q., Ahrlund Richter, L., Auerbach, J.M., Benvenisty, N., Charo, R.A., Chen, G., Deng, H.K., Goldstein, L.S., Hudson, K.L., Hyun, I., et al. (2007). Ethics. The ISSCR guidelines for human embryonic stem cell research. Science 315, 603-604.
- 56. Hyun, I., Clayton, E.W., Cong, Y., Fujita, M., Goldman, S.A., Hill, L.R., Monserrat, N., Nakauchi, H., Pedersen, R.A., Rooke, H.M., et al. (2021). ISSCR guidelines for the transfer of human pluripotent stem cells and their direct derivatives into animal hosts. Stem Cell Rep. 16, 1409-1415.
- 57. Fujimoto, T., Yamanaka, S., Tajiri, S., Takamura, T., Saito, Y., Matsumoto, N., Matsumoto, K., Tachibana, T., Okano, H.J., and Yokoo, T. (2020). Generation of Human Renal Vesicles in Mouse Organ Niche Using Nephron Progenitor Cell Replacement System. Cell Rep. 32, 108130.
- 58. Hu, Z., Li, H., Jiang, H., Ren, Y., Yu, X., Qiu, J., Stablewski, A.B., Zhang, B., Buck, M.J., and Feng, J. (2020). Transient inhibition of mTOR in human

- pluripotent stem cells enables robust formation of mouse-human chimeric embryos. Sci. Adv. 6, eaaz0298.
- 59. Ludwig, T.E., Bergendahl, V., Levenstein, M.E., Yu, J., Probasco, M.D., and Thomson, J.A. (2006). Feeder-independent culture of human embryonic stem cells. Nat. Methods 3, 637-646.
- 60. Zhang, B., Li, H., Hu, Z., Jiang, H., Stablewski, A.B., Marzullo, B.J., Yergeau, D.A., and Feng, J. (2021). Generation of mouse-human chimeric embryos, Nat. Protoc. 16, 3954-3980.
- 61. Schrode, N., Saiz, N., Di Talia, S., and Hadjantonakis, A.K. (2014). GATA6 levels modulate primitive endoderm cell fate choice and timing in the mouse blastocyst. Dev. Cell 29, 454-467.
- 62. Joyner, A., and Wall, N. (2008). Immunohistochemistry of whole-mount mouse embryos. CSH Protoc. pdb prot4820.
- 63. Rigueur, D., and Lyons, K.M. (2014). Whole-mount skeletal staining. Methods Mol. Biol. 1130, 113-121.
- 64. Truett, G.E., Heeger, P., Mynatt, R.L., Truett, A.A., Walker, J.A., and Warman, M.L. (2000). Preparation of PCR-quality mouse genomic DNA with hot sodium hydroxide and tris (HotSHOT). Biotechniques 29, 52-54.
- 65. Kim, D., Paggi, J.M., Park, C., Bennett, C., and Salzberg, S.L. (2019). Graph-based genome alignment and genotyping with HISAT2 and HISAT-genotype. Nat. Biotechnol. 37, 907-915.
- 66. Liao, Y., Smyth, G.K., and Shi, W. (2014). featureCounts: an efficient general purpose program for assigning sequence reads to genomic features. Bioinformatics 30, 923-930.
- 67. Robinson, M.D., McCarthy, D.J., and Smyth, G.K. (2010). edgeR: a Bioconductor package for differential expression analysis of digital gene expression data. Bioinformatics 26, 139-140.
- 68. Yu, G., Wang, L.G., Han, Y., and He, Q.Y. (2012). clusterProfiler: an R package for comparing biological themes among gene clusters. OMICS 16, 284-287.
- 69. Lin, G., Martins-Taylor, K., and Xu, RH. (2010). Cellular Programming and Reprogramming. Methods in Molecular Biology. Humana Press 636. https://doi.org/10.1007/978-1-60761-691-7\_1.
- 70. Love, M.I., Huber, W., and Anders, S. (2014). Moderated estimation of fold change and dispersion for RNA-seq data with DESeq2. Genome Biol. 15, 550. https://doi.org/10.1186/s13059-014-0550-8.
- 71. Shifu, C., Yanqing, Z., Yaru, C., and Jia, G. (2018). fastp: an ultra-fast all-inone FASTQ preprocessor. Bioinformatics 34, i884-i890. https://doi.org/ 10.1093/bioinformatics/bty560.
- 72. Zhang, Y., Yi, Y., Xiao, X., Hu, L., Xu, J., Zheng, D., Koc, H.C., Chan, U.I., Meng, Y., Lu, L., et al. (2023). Definitive Endodermal Cells Supply an in vitro Source of Mesenchymal Stem/Stromal Cells. Commun Biol. 6, 476. https://doi.org/10.1038/s42003-023-04810-5.



### **STAR**\***METHODS**

### **KEY RESOURCES TABLE**

REAGENT or RESOURCE	SOURCE	IDENTIFIER
Antibodies		
FITC goat polyclonal anti-GFP	Abcam	ab6662; RRID: AB_305635
Rabbit polyclonal anti-GFP	Invitrogen	A-6455; RRID: AB_221570
Mouse monoclonal anti-GFP	ProteinTech	66002-1-lg; RRID: AB_11182611
Rabbit polyclonal anti-cleaved caspase3	CST	9661S; RRID: AB_2341188
Mouse monoclonal anti-human BCL2	BD Biosciences	51-6511GR
Rabbit polyclonal anti-BCL-XL	ProteinTech	26967-1-AP; RRID: AB_2880702
Recombinant Alexa Fluor® 568 Anti-CD90	Abcam	ab201848
Rabbit polyclonal anti-NANOG	ProteinTech	14295-1-AP; RRID: AB_1607719
Rabbit polyclonal anti-OCT4	Invitrogen	PA5-27438; RRID: AB_2544914
Rabbit monoclonal anti-Cdx2	Abcam	ab76541; RRID: AB_1523334
Mouse monoclonal anti-Gata3	Thermo Fisher	MA1-028; RRID: AB_2536713
Rabbit polyclonal anti-Sox9	Milipore	AB5535; RRID: AB_2239761
Mouse monoclonal anti-α-SMA, Alexa Fluor 488	eBioscience <sup>TM</sup>	53-9760-82; RRID: AB_2574461
Cytokeratin Pan Type I/II antibody	Thermo Fisher	MA5-13156; RRID: AB_10983023
Rabbit monoclonal anti-Sp7/Osterix	Abcam	ab209484; RRID: AB_2892207
Rabbit monoclonal anti-PDGFRα	Abcam	AB203491; RRID: AB_2892065
Alexa Fluor® 488 mouse anti-human Vimentin	BD Biosciences	562338; RRID: AB_10896994
Mouse monoclonal anti-GAPDH	Abclonal	AC002; RRID: AB_2736879
Rabbit monoclonal anti-β-actin	Abclonal	AC038; RRID: AB_2863784
Donkey anti-Mouse IgG (H + L) Highly Cross-Adsorbed Secondary Antibody, Alexa Fluor 488	Invitrogen	A-21202; RRID: AB_141607
Donkey anti-Rabbit IgG (H + L) Highly Cross-Adsorbed Secondary Antibody, Alexa Fluor 488	Invitrogen	A-21206; RRID: AB_2535792
Goat anti-Rabbit IgG (H + L) Cross- Adsorbed Secondary Antibody, Alexa Fluor 546	Invitrogen	A-11010; RRID: AB_2534077
Donkey anti-Mouse IgG (H + L) Highly Cross-Adsorbed Secondary Antibody, Alexa Fluor 594	Invitrogen	A-21203; RRID: AB_141633
Donkey anti-Rabbit IgG (H + L) Highly Cross-Adsorbed Secondary Antibody, Alexa Fluor 594	Invitrogen	A-21207; RRID: AB_141637
Donkey anti-Rabbit IgG (H + L) Highly Cross-Adsorbed Secondary Antibody, Alexa Fluor 647	Invitrogen	A-31573; RRID: AB_2536183
Donkey anti-Mouse IgG (H + L) Highly Cross-Adsorbed Secondary Antibody, Alexa Fluor 647	Invitrogen	A-31571; RRID: AB_162542
Chemicals, peptides, and recombinant proteins		
PMSG	Prospec	HOR-272
nCG	Sigma	C1063
M2 medium	Sigma	M7167
x-MEM	Gibco	12571071

(Continued on next page)



Continued		
REAGENT or RESOURCE	SOURCE	IDENTIFIER
Progesterone	Sigma	P0130
β-estrodial	Sigma	E8875
GlutaMax	Invitrogen	35050061
NEAA	Gibco	11140050
2-Mercaptoethanol	Sigma	63689
Puromycin	ACROS	58-58-2
Rock inhibitor, Y27632	Tocris	1254
Penicilin-Streptomycin	Thermo	10378016
TrypLE	Thermo	12605010
mTeSR1 medium	Stem Cell Technologies	5870
EDTA	sigma	E5134
TS-X	Gibco	51500056
DPBS	Gibco	14190250
4% Paraformaldehyde (PFA)	Sigma	158127
Sucrose	FLUKA	84100
FBS	Gibco	26140079
BSA	Sigma	A7030
Triton X-100	Sigma	93443
Tyrode's solution	Sigma	T1788
4', 6-diamidino-2-phenylindole (DAPI)	Sigma	D9542
Alcian blue	Sigma	A5268
Alizarin red	-	A5533
Oil Red O	Sigma	O0625
	Sigma	A6283
Glacial acetic acid	Sigma	32221
Ethanol	Sigma	
Potassium hydroxide	ACROS	1310-58-3 179124
Acetone	Sigma	179124
Critical commercial assays	Otto -	A4007404
Chondrogenesis Differentiation kit	Gibco	A1007101
Adipogenesis Differentiation kit	Gibco	A1007001
Osteogenesis Differentiation kit	Gibco	A1007201
Human MSC characterization kit	BD	562245
Vybrant Multicolor Cell Labeling Kit	Life Technologies	V22889
OneTaq HotStart Master Mix	NEB	M0488
RIPA buffer	Thermo Scientific	89901
Protease inhibitor cocktail	Sigma	P-8465
Bovine serum albumin standard set	Bio-rad	500-0207
Western ECL Substrate	Bio-rad	170–5061
Deposited data		
Raw and analyzed data	This paper	GEO: GSE195573
Experimental models: Cell lines		
Human: ESCs (Envy)	Costa et al., 2005 <sup>34</sup>	N/A
Human: ESCs (CT3)	Ge et al., 2010 <sup>56</sup>	N/A
Experimental models: Organisms/strains		
<u> </u>		040
Mouse/C57BL/6J	Charles River	219
	Charles River Charles River	
Mouse/C57BL/6J Mouse/CD-1 (ICR) Mouse/Prx1-Cre		219 201 005584

(Continued on next page)



Continued		
REAGENT or RESOURCE	SOURCE	IDENTIFIER
Mouse/FVB	Charles River	215
Oligonucleotides		
Oligonucleotides are summarized in Table S1	This study	N/A
shRNA sequences are summarized in Table S1	This study	N/A
Recombinant DNA		
pLv224-EF1α-BCL2-IRES2- GFP-IRES-Puro	GeneCopoeia	https://www.genecopoeia.com/ wp-content/uploads/oldpdfs/ tech/omicslink/pReceiver-Lv224.pdf
pLVRU6GP-U6-shRNA-SV40- eGFP-IRES-Puro	GeneCopoeia	https://www.genecopoeia.com/ wp-content/uploads/oldpdfs/ product/shrna/psi-LVRU6GP.pdf
Software and algorithms		
Prism 9	GraphPad Software	https://www.graphpad.com/ scientific-software/prism/
FlowJo	BD	https://www.flowjo.com/solutions/flowjo
ZEN 2012	Zeiss	N/A
NIS-Elements	Nikon	N/A
fastp	Chen, Zhou et al. 2018 <sup>57</sup>	https://github.com/OpenGene/fastp
HISAT2	Kim, Paggi et al. 2019 <sup>58</sup>	http://daehwankimlab.github.io/hisat2/
featureCounts	Liao, Smyth et al. 2014 <sup>59</sup>	http://subread.sourceforge.net/
DESeq2	Love, Huber et al. 2014 <sup>60</sup>	https://bioconductor.org/packages/release/bioc/html/DESeq2.html
edgeR	Robinson, McCarthy et al. 2010 <sup>61</sup>	https://bioconductor.org/packages/ release/bioc/html/edgeR.html
clusterProfiler	Yu, Wang et al. 2012 <sup>62</sup>	https://bioconductor.org/packages/ release/bioc/html/clusterProfiler.html

### **RESOURCE AVAILABILITY**

### **Lead contact**

Further information and requests for resources and reagents should be directed to and will be fulfilled by the lead contact, Ren-He Xu (renhexu@um.edu.mo).

### **Materials availability**

This study did not generate new unique reagents.

### Data and code availability

- Data: Data have been deposited at NCBI GEO and are publicly available as of the date of publication. Accession numbers are listed in the key resources table.
- Code availability: This paper does not report original code.
- Any additional information required to reanalyze the data reported in this paper is available from the lead contact upon request.

### **EXPERIMENTAL MODEL AND STUDY PARTICIPANT DETAILS**

### **Ethics statement**

This study strictly followed the International Society for Stem Cell Research guidelines for studies on hESCs 63,64, and the ethics protocol #BSERE19-APP026-FHS approved by the University of Macau Panel on Research Ethics, which allowed human-mouse chimeras to develop until E14-E16. We also referred to several human-mouse chimeric studies in which the chimeras were developed until E13.5<sup>65</sup> or even E17.5<sup>66</sup> and no human cells integrated in the central nervous system or gonads. Animal experiments in this study followed the amended version of the animal use protocol #UMARE-030-2019 approved by the University of Macau Animal Research Ethics Sub-panel.





Male and female C57BL/6J mice, raised in the University of Macau Animal Research Core, were used to produce wild-type (WT) blastocysts, and male  $Prrx1^{Cre}$  mice and female  $Sox9^{flox/flox}$  mice, purchased from the Jackson Laboratory, were crossed to produce Sox9\*/- blastocysts. The blastocysts were used for microinjection with donor cells. ICR (CD-1) female mice were used for surrogacy of the injected blastocysts. All mice were maintained in the animal research core and tested to be free for specific pathogens.

### **METHOD DETAILS**

### **hESC** culture and MSC generation

The Envy (GFP+)<sup>34</sup> hESC line was used in this study. hESCs were cultured in mTeSR1 medium and passaged every 5–7 days.<sup>67</sup> EMSCs including were generated by inducing hESCs to differentiate into MSC via trophoblasts or NC cells following our own protocol<sup>24</sup> and others' protocol,<sup>39</sup> respectively. Specifically for EMSCs, hESCs were induced to trophoblast as intermediate stage by adding BMP4(10 ng/mL) and 1 μM A83-01 in mTeSR1 medium minus selected factor (Stem Cell Technologies) for 5 days. Then complete MSC medium (α-MEM supplemented with 20% fetal bovine serum, 1x L-glutamine and 1x nonessential amino acids) was used to differentiate trophoblast-like cells to MSCs for two weeks. Medium was replaced every other day. Cells were passaged once reached full confluency every 5-7 days through TrypLE (Gibco) digest. For NC-EMSCs derivation in brief, hESCs were seeded in mTeSR1 medium for overnight attachment. Cells were applied with neural crest induction medium, composing of 1 μM dorsomorphin (Selleck), 1 μM CHIR99021 (Selleck), 10 μM SB431542 (Selleck), 10 ng/mL bFGF (Thermo), and 22.5 ng/mL sodium heparin (Sigma) in Essential 6 (E6) medium (Gibco) for 15 days. Cells was split in 1-6 manners when reached full confluency. Then complete MSC medium was applied for further 10 days induction to complete full NC-EMSCs derivation.

All MSCs were cultured in complete MSC medium containing 20% fetal bovine serum, 1x NEAA and 1x GlutaMax in α-MEM (Gibco BRL, Grand Island, NY, USA) at 37°C with 5% CO2. MSCs were passaged every 3-5 days when confluency reached more than 90%, using 1x TrypLE for 5-min incubation followed by seeding of 15% of resuspended cells in a new culture plate. The cells were verified for typical MSC markers via flow cytometry and trilineage differentiation and used in this study before they reached passage 5.

### Blastocyst isolation and microinjection

Superovulation, mating, and blastocyst retrieval were performed as described previously. 68 In brief, female mice (3-4 weeks old) were superovulated through i.p. injection with 5 IU of pregnant mare serum gonadotropin (PMSG) and 48 h later with 5 IU of human chorionic gonadotropin (hCG). After 1:1 pairing with male mice, vaginal plugs were checked the next morning, which is designated as 0.5-day post coitum (dpc). Blastocysts were retrieved from the uterine horns of plugged females at 3.5 dpc and washed in prewarmed M2 medium. The embryos that possess obvious blastocoel were regarded as timely developed blastocysts.

Cells that need to be injected were dissociated, singularized, and resuspended in M2 medium. Individual cells were loaded into a micropipette (20 µm inner diameter). 10-15 cells were delivered to the cavity of each blastocyst. The injected blastocysts were kept in warm M2 medium before being transferred to in vitro culture for live imaging or to surrogate hosts.

### **Embryo implantation**

Adult ICR female mice in estrus were mated with vasectomized adult male in 1:1 pairing to achieve pseudopregnancy. Vaginal plugs were checked the next morning after mating and the time is designated as 0.5 dpc. Plugged female mice were used as surrogate host for embryo implantation. Embryo transfer was performed on properly anesthetized pseudopregnant ICR mice at 2.5 dpc. First, injected blastocysts were loaded into a glass pipette and transferred to both uterine horns of the surrogates with 10~12 embryos per horn. Each surgery was finished within 20 min per surrogate and the operated animals were kept warm via heating until they woke up from anesthetization.

### In vitro culture of mouse embryos

Mouse blastocysts were cultured in the *in vitro* culture medium IVC for short-term development *in vitro* as reported.<sup>36</sup> Briefly, 20% FBS, glutaMax, penicillin/streptomycin, 1xlTS-X, β-estradiol, progesterone, and N-acetyl-L-cysteine were added to DMEM/F12, which was then filtered for use. Micro-drops of the IVC medium (1 µL per drop) were aligned on the bottom surface of confocal dish and immersed with sterile mineral oil to prevent evaporation. One to four embryos were transferred to the middle of each drop using mouth pipette. Embryos were cultured in the IVC medium for up to 14 h at 37°C and photographed under Zeiss inverted fluorescence microscope accessed with incubating chamber and humidifier.

### Whole-mount embryo staining and imaging

The immunofluorescence of whole-mount pre-implantation embryos was performed as previously described. <sup>69</sup> In brief, embryos were incubated in Tyrode's Acid (TA) solution at 37°C to remove the zona pellucida. Then they were fixed in 4% paraformaldehyde (PFA) for 10 min at room temperature (RT) and permeabilized in 1% Triton X-100 for 15 min. The fixed samples were washed twice with PBS using glass pipette before each transfer to a different solution and incubated in the Blocking Buffer containing 20% FBS and 0.1% Triton X-100 in PBS at RT for 1 h. Primary antibodies were added to the Staining Buffer containing 3% BSA in PBS for incubation



at 4°C overnight. After washing with PBS at least three times, fluorophore-conjugated secondary antibodies were added to fresh Staining Buffer for 2-h incubation in dark. 4', 6-diamidino-2-phenylindole (DAPI) was applied right before imaging. Micro-drops of PBS (0.5 μL each) were arrayed on the bottom surface of a confocal dish and immersed with mineral oil. 1–3 embryos were transferred into each drop and placed with the ICM aside and blastocoel front. Images were taken under a Nikon A1R laser scanning confocal microscope.

### Histological analysis

Tissues were fixed in 4% PFA at 4°C overnight. After washing at least three times, sucrose solution was used to dehydrate samples. Optimal cutting temperature (OCT) compound was used to immerse and embed samples to prepare for cryo-section. OCT compound was washed away by double distilled water (ddH<sub>2</sub>O). Sections were stained with hematoxylin and eosin (H&E) for light microscopic imaging. For immunofluorescence, after washing away OCT, 1% Triton X-100 in PBS was used to permeabilize samples and antigen retrieval was performed using the heating method with a citrate buffer. Dections were blocked in 3% BSA at RT for 1.5 h and incubated with primary antibodies at 4°C overnight. After washing at least three times, fluorophore-conjugated secondary antibodies were applied and incubated at RT for 2 h. After removing residual antibodies via PBS washing, sections were mounted with a DAPI solution for nuclear counterstaining and imaging.

### Whole-mount skeleton staining

The whole skeleton of mouse fetuses was stained as reported. 71 In brief, mouse fetuses were isolated with forceps by separating from maternal and extraembryonic tissues under light microscope. The exposed fetuses were washed with PBS to remove blood and amniotic fluid, and then fixed in 70% ethanol at 4°C overnight. Fixed fetuses were transferred into 95% ethanol for 1 h and at RT before being placed into acetone for overnight incubation at 4°C. Samples were placed in the Alcian blue Solution containing 0.03% Alcian blue in 80% EtOH and 20% glacial acetic acid for one day at RT, and then in Alizarin Red Solution containing 0.005% Alizarin red and 1% KOH in distilled water for 16 h at room temperature. Stained samples were cleared and transparentized in 1% KOH at RT for at least 1 day, of which the duration depended on the development of transparency of the samples. The transparent specimens were transferred to the Imaging Buffer containing 1% KOH and glycerol in 1:1 ratio for light microscopy.

### Genotyping

For the mouse founder strains Sox9<sup>flox/flox</sup> and Prrx1<sup>Cre</sup>, genotyping was performed via polymerase chain reaction (PCR) on genomic DNA isolated from the mouse tails. For Prrx1<sup>Cre</sup>:Sox9<sup>+/-</sup> fetuses, genotyping was performed via PCR on genomic DNA isolated from the yolk sac. The isolated tissues were lysed in a heating alkaline buffer for DNA extraction. 72 The primers used are listed in the Table S1.

### **Knockdown assay with lentiviral vectors**

Four pairs of short-hairpin (sh) RNA targeting human BCL2 and one pair of scrambled shRNA were designed, synthesized, and constructed into the lentiviral vector psi-LVRU6GP-U6-shRNA-EF1α-eGFP-IRES-Puro (GeneCopoeia). The shRNA-expressing vector and viral packaging vectors pCMVR8.74 (Addgene #22036) and pMD2.G (Addgene #12259) were used to transfect 293FT cells to generate lentiviral particles. MSCs were seeded onto flatten adhering plates and transduced with lentiviral particles when confluency reached 80%. Puromycin selection (1 μg/mL in the MSC Medium) was conducted on the transduced cells for one week.

### **Western blotting**

Cells were lysed in the radioimmunoprecipitation assay (RIPA) Buffer including protease/phosphatase inhibitors (Sigma). Lysed cells in the buffer were gently shaken and incubated on ice for ½ h, and then centrifugated to collect the supernatant. Protein concentrations were determined by using the Bradford assay (Bio-Rad). 15 µg of proteins per sample was loaded into each well of a sodium dodecyl sulphate-polyacrylamide gel (Bio-Rad). Semi-dry transfer of proteins from the gel to a polyvinylidene fluoride (PVDF) membrane (Milipore) was performed and blocked in the Blocking Buffer containing 5% milk and 0.1% Triton X-100 for 1 h and at RT. The blocked membrane was incubated with primary antibodies at 4°C overnight and then secondary antibodies at RT for 1 h with washing 3 times before each transfer to a new solution. Chemiluminescent signals were detected under the ChemiDoc Imaging System (Bio-Rad).

### **Trilineage differentiation of MSCs**

For adipogenesis and osteogenesis, MSCs were seeded in a flat culture plate and induced for differentiation when the cell confluency reached 60% and 90% respectively, using the StemPro Adipogenesis and Osteogenesis Differentiation Kit (Life Technologies). For chondrogenesis, MSCs were seeded to a low-attachment U-bottom plate to form spheroids, and then induced for differentiation using the StemPro Chondrogenesis Lit (Life Technologies). Adipocyte differentiation was stopped at day 30 and the resultant samples were stained with Oil Red O. Osteocyte and chondrocyte differentiation were terminated at day 14 and stained with Alizarin red and Alcian blue, respectively. Imaging was conducted under light microscope.





### Flow cytometry

MSCs were dissociated with TrypLE and washed with 1% FBS in pre-chilled PBS. Cells were incubated with fluorophore-conjugated antibodies in the Staining Buffer containing 2% FBS in PBS on ice for ½ h. Then cells were washed twice with pre-chilled PBS containing 1% FBS and analyzed on the Beckman Coulter Cytoflex. Antibodies are listed in the key resource table.

### **Bulk RNA-seq and analysis**

Embryos were firstly lysed in lysis buffer (Triton X-100, dNTPs, and RNase in ultrapure H2O), then amplified, reversely transcribed, and prepared libraries for SMART V4-seq. The adapter sequences and short reads under 20 bp were filtered by fastp (Chen, Zhou et al. 2018). We used HISAT2<sup>58</sup> version 2.2.1 for alignment to human genome (hg38). Gene counts were generated by feature-Counts<sup>59</sup> version 2.0.1. For comparisons of EMSCs (0 h), blastocysts injected with EMSCs and cultured for 6 h and 14 h, Differentially expressed genes (DEGs) were determined by edgeR<sup>61</sup> version 3.32.1 without replication model. All the significantly changed genes were selected with the cut-off adjust p-value <0.001 and |fold change| > 1. GO enrichment were analyzed using clusterProfiler<sup>62</sup> version 4.1.4 with default parameters. Top-10 GO terms were selected at level 5 for visualization.

### **QUANTIFICATION AND STATISTICAL ANALYSIS**

All quantitative data are presented as the mean  $\pm$  SEM. Experiments were repeated at least three times with repeat number indicated as "n" in the figure legends. Statistical analyses were conducted by using a t test analysis with Prism (GraphPad Software). p values less than 0.05 were considered statistically significant. The statistical difference was labeled with the signs as \* for p < 0.05, \*\*p < 0.01, \*\*\*p < 0.001, and n.s. not significant.